

# Maximizing heat recovery in an air-to-air heat exchanger by monitoring heat transfer

M. R. L. BANTLE<sup>1</sup>, E. M. BARBER<sup>2</sup>, S. SOKHANSANJ<sup>2</sup>, and E. B. MOYSEY<sup>2</sup>

<sup>1</sup>*Bantle Engineering Research, P.O. Box 7805, Saskatoon, SK, Canada S7K 4R5; and* <sup>2</sup>*Department of Agricultural Engineering, University of Saskatchewan, Saskatoon, SK, Canada S7N 0W0. Received 1 March 1988, accepted 10 March 1989.*

Bantle, M. R. L., Barber, E. M., Sokhansanj, S., and Moysey, E. B. 1989. **Maximizing heat recovery in an air-to-air heat exchanger by monitoring heat transfer.** *Can. Agric. Eng.* **31**: 217-225. One of the greatest problems associated with the use of heat exchangers in livestock buildings is the accumulation of frost in the exhaust air passages under cold supply air conditions. In this project, a frost control system was developed in which the rate of heat transfer was monitored and used to control the rate of frost accumulation and to schedule a defrost cycle. Results are reported for both computer simulations and for experiments with a 472 L/s heat exchanger that employed the new control system. The experiments were conducted for a supply air temperature of  $-25^{\circ}\text{C}$ , and for exhaust air temperatures and relative humidities of 13 and  $25^{\circ}\text{C}$ , and 40 and 75%, respectively. The results showed that the rate of heat recovery was less than the maximum thermodynamic recovery potential for the heat exchanger but greater than that attainable without a defrost cycle. A theoretical analysis suggested that the heat-transfer based control strategy has the potential to improve the overall heat recovery compared to time or pressure-based defrost control systems.

## INTRODUCTION

Experience has shown that air-to-air heat exchangers can be successfully used in Canadian livestock buildings. In many cases, their use makes provision of other sources of heat unnecessary. The greatest problem associated with the use of heat exchangers is the accumulation of frost in the exhaust air passages when the supply air is very cold. The problem is especially severe in livestock barns where the exhaust air may be cool and humid. This paper reports on the development of a frost control system in which the rate of heat transfer is monitored and used to control the rate of frost accumulation and to schedule the defrost cycles.

## ALTERNATIVE FROST CONTROL STRATEGIES

One possible frost control strategy involves using very large air passages such that complete blockage with frost will not occur (Meyer et al. 1983); This alternative is not appropriate in applications requiring compact heat exchangers. Furthermore, the effectiveness of the heat exchanger will be progressively reduced as frost accumulation increases.

A second alternative is to prevent the formation of frost by maintaining the exchanger core temperature above  $0^{\circ}\text{C}$ . Control over the core temperature can be accomplished by pre-heating the supply air or by imbalancing the air flow rates. The potential for heat recovery is severely limited by this alternative when the barn air temperature is very cool, say  $10^{\circ}\text{C}$ , as might be experienced in a dairy barn.

Bantle (1986) developed and tested a third alternative in which frost was allowed to form but not to accumulate beyond the level at which the rate of heat transfer is significantly reduced. He reported results of computer simulations and of a laboratory experiment with a full-scale heat exchanger showing that this alternative was not feasible. Once frost began to accumulate on the core surfaces, the frost layer continued to grow for any

core temperature below  $0^{\circ}\text{C}$ . Frost build-up could not be controlled satisfactorily by adjusting the supply air flow rate. After 6 h of use, the frost could only be removed by defrosting the core, which required that all the supply air be bypassed. His work suggested that maximum heat recovery could only be obtained by a cycle of frost accumulation followed by a defrost.

## DEFROST CONTROL ALTERNATIVES

To initiate defrost of a frosted core, the flow of supply air to the core can be reduced or stopped or, in some cases, the supply fan can be reversed to cause warm exhaust air to pass through the cold side of the core. Several schemes have been employed to schedule the defrost cycle, including manual operation, timers, and pressure monitors. Manual defrost, while appealing because of its simplicity and low cost, is difficult if it is necessary to defrost more than once a day. Timed defrost control systems are relatively simple and inexpensive but they are difficult to optimize for all conditions. Defrost cycles may occur too infrequently during cold weather and too often during warm weather. Pressure-based systems initiate a defrost when the static pressure differential across the exhaust side of the heat exchanger exceeds a set point value. The defrost is complete when the static pressure differential returns to normal. The set points for a pressure controller must be determined for each heat exchanger model, presumably at the factory. Pressure sensors and the associated monitors are, at the present time, expensive. Also, if the exhaust air passages of the heat exchanger become fouled, the pressure drop across an unfrosted core could rise significantly so that the present value was not achieved, thereby rendering the controller inoperative.

No references were found in the literature to studies in which the defrost cycle of a heat exchanger was scheduled on the basis of a declining rate of heat transfer. Consider the heat exchanger configuration shown in Fig. 1. Following a defrost, maximum flow of fresh supply air could be directed through the core. The temperature difference between air entering and leaving the supply side of the core could be used to calculate the maximum rate of heat recovery. The mass flow rate would remain constant and the air temperatures would be monitored continuously. When the temperature difference, and hence the rate of heat transfer, was reduced by a preset amount, a defrost cycle could be initiated by bypassing all of the supply air.

In the above-described simple control strategy, the decline in the rate of heat transfer is used to schedule a defrost, but the rate of heat transfer is not controlled. However, in a more generalized control scheme, the proportion of supply air passing through the core could be varied to levels other than 0 and 100%. This modulation of the supply air stream would provide control over the rate of heat transfer and hence over the rate of formation and accumulation of frost. By monitoring the rate of heat transfer, the potential would exist to optimize the overall heat recovery rate automatically as air stream conditions change or as the core becomes fouled with foreign materials.

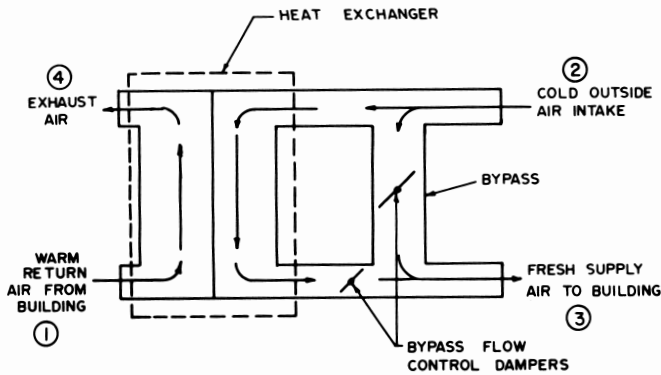


Table I. Heat exchanger physical data†

Spacing between exchanger surfaces	5.4 mm
Assumed dry surface fouling factor	0.0 m <sup>2</sup> K/W
Thickness of exchanger surfaces ‡	0.152 mm
Thermal conductivity of core‡	208 W/m K
Length of exchanger surfaces	0.880 m
Width of exchanger surfaces	0.408 m
Number of hot passages	49
Number of cold passages	50
Number of heat exchange surfaces	98

† Measured unless otherwise noted.

‡ Private communication with manufacturer.

Figure 1. Schematic of heat exchanger with flow control dampers.

### OBJECTIVES

The objective of this work was to develop and test a control algorithm in which the rate of heat transfer is continuously measured and controlled and in which a defrost cycle is scheduled on the basis of a decline in the rate of heat transfer. A further hypothesis to be tested was that a defrost cycle will increase the time averaged heat transfer rate compared to a control system in which the coldest part of the heat exchanger core is maintained at 0°C. The objectives were to be accomplished using both a computer model of a frosting heat exchanger and laboratory tests with an experimental heat exchanger operating under conditions typical of livestock barns in cold climates.

### EXPERIMENTAL PROCEDURE

#### Experimental apparatus and experimental conditions

The heat exchanger selected for the tests was a 470 L/s capacity plate type counterflow commercial heat exchanger. The physical characteristics of the heat exchanger are given in Table I and the heat exchanger overall dimensions are shown in Fig. 2.

Accumulation of frost in the heat exchanger was controlled by reducing the supply of cold air to the heat exchanger. A modulating damper system (Fig. 1) was used to control the amount of outside air which bypassed the core.

Test conditions selected for the four experimental runs are shown in Table II. The values for the exhaust air temperature and relative humidity were selected to bracket the range of conditions often encountered in livestock buildings in cold climates.

Run duration was selected to provide at least three complete controller cycles; whereas longer duration runs would have been desirable, repeating the control cycle three times was considered sufficient to demonstrate continuous operation of the controller. Replication of complete runs was considered unnecessary since all of the parameters affecting heat transfer either were fixed for all runs or were measured or controlled.

The arrangement of the test equipment is shown in Fig. 3. Air which was to be exhausted entered the heat exchanger through the conditioning box (5) where the relative humidity and temperature were adjusted to test requirements. The air then passed through the fan (3) to boost the static pressure.

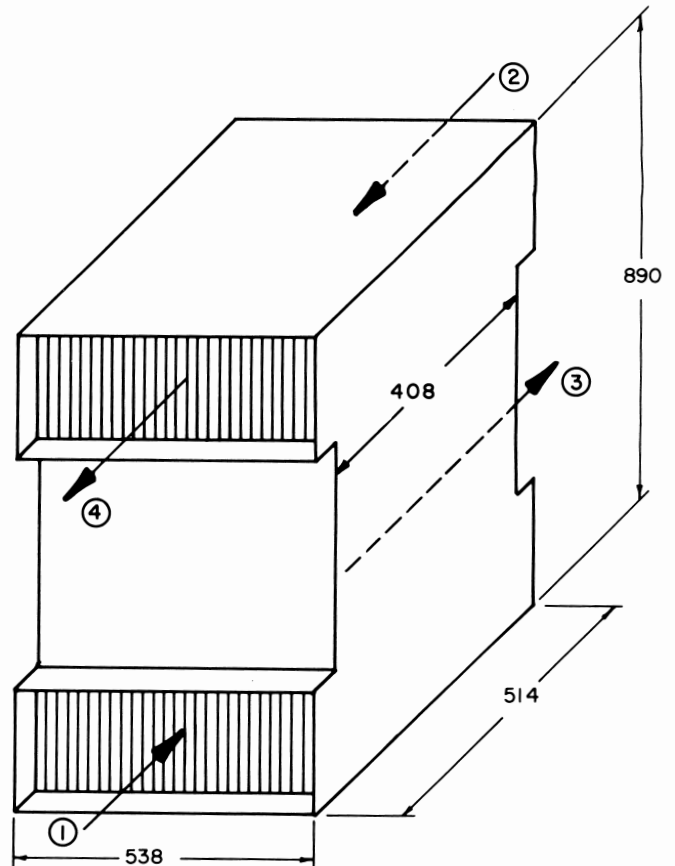


Figure 2. Heat exchanger dimensions and configuration.

Wet-bulb and dry-bulb temperatures were measured in a psychrometric box (4) and air volume flow rate was measured by a nozzle station (2). The air then passed through a straight section of duct to a temperature measurement section (12) where eight individual temperatures were measured on an equal area grid. The air then passed through the exhaust side of the heat exchanger (1). After exiting the heat exchanger the air passed through a second temperature measurement section (12). A sample was drawn into a psychrometric box where the wet-bulb and dry-bulb temperature of the air were measured (4). The cooled air was then exhausted back into the laboratory.

Cold air entered on the supply side from a controlled environment room at (6). This cold air could proceed either through the bypass or through the heat exchanger. Air going to the heat exchanger entered a flow tube (9) where the mass flow rate was

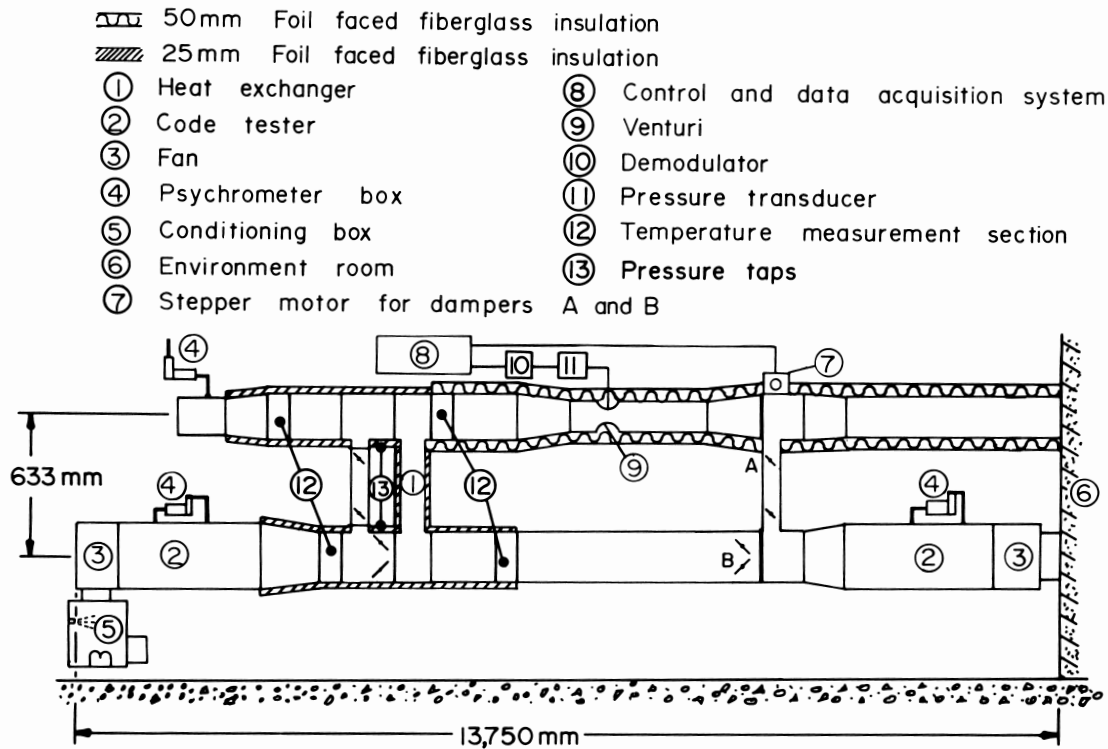


Figure 3. Experimental apparatus.

Table II. Averaged conditions during four test runs

Parameters	Units	Run 1	Run 2	Run 3	Run 4
Maximum supply air flow rate	kg/s	0.43	0.44	0.45	0.45
Supply air temperature at inlet	°C	-24	-25	-27	-26
Supply air relative humidity at inlet†	%	100	100	100	100
Exhaust air flow rate	kg/s	0.31	0.32	0.33	0.33
Exhaust air temperature at inlet	°C	24	25	13	13
Exhaust air relative humidity at inlet	%	78	42	77	46
Test duration	h	4.5	8.0	7.0	10.0
Atmospheric pressure	kPa	93.2	94.4	95.2	95.1

†Air was delivered from a refrigerated air supply and was assumed to be 100% relative humidity.

accurately measured using a venturi meter. The air passed through a temperature measurement section (12) both before and after going through the supply side of the heat exchanger

(1). After passing through a long section of duct this air was mixed with the air from the bypass. The mixed air was drawn through a nozzle station (2) by a fan (3) and exhausted back into the environment room (6).

Where control of air flow is by means of dampers, it is unlikely that linear operation of the damper will produce a linear change in air flow rate. Figure 4 shows one series of measurements of mass flow through the supply side of the heat exchanger as a function of the damper system position. This series of measurements confirmed the nonlinearity of the damper system and indicated that problems could be expected to occur if control actions were to be attempted in the range from step 170 to step 240.

Air temperatures at the temperature measurement sections (12) were measured using an integrated circuit temperature transducer which produced an output current proportional to absolute temperature. The mean air temperature at a section was calculated by averaging the temperatures measured by eight sensors placed on an equal area grid. Measurements of the velocity profiles at these sections indicated that averaging the eight temperature measurements gave an accurate air stream average temperature.

Wet-bulb and dry-bulb temperatures were measured in psychrometric boxes (4) using Type T thermocouples. Whereas the measured temperatures of the inlet exhaust air stream were found to be accurate, tests indicated that the temperature measurements of the exit exhaust air stream were not as accurate. In some of the runs, liquid droplets in the air stream appeared to have interfered with the dry-bulb temperature measurements. Since measurements from the exhaust side were not required

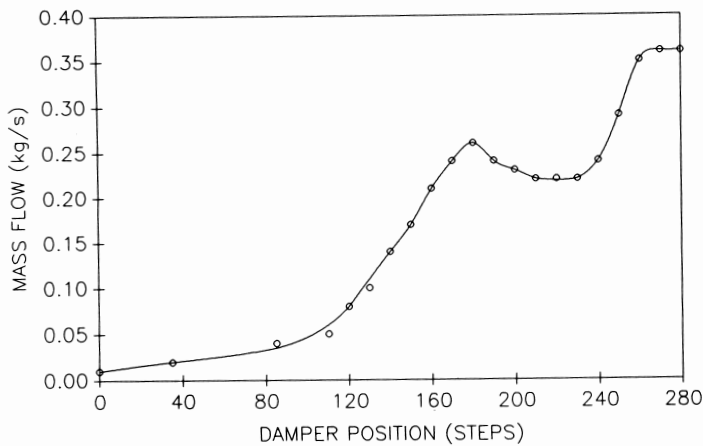


Figure 4. Flow characteristics of damper.

for programming the controller, errors did not affect controller operation. The humidity ratio of the supply air stream was constant and was assumed equal to the humidity ratio of saturated air at the supply air inlet temperature.

The core temperature was computed by averaging the temperatures measured by three thermocouples mounted on the core in the cold air passages of the heat exchanger. These sensors were mounted such that they were measuring the coldest core temperatures within the heat exchanger.

The entire heat exchanger and ducts were insulated to prevent heat loss that would introduce errors in measurement of the mass flow rate and of the various air temperatures. The maximum error in mass flow rate measurement on the supply side due to heat loss through the ducts was calculated to be 0.2%.

The pressure drop across the heat exchanger core on the exhaust side was measured as an indication of the amount of frost accumulation. Two pressure taps were placed in the duct immediately upstream and downstream of the exhaust side of the core. Pressure measurements were recorded manually at 30-m intervals during each run. Also, as an indication of the extent of frost accumulation, condensate that drained from the core was weighed.

The control and data acquisition system consisted of a computer controller board, a 12 bit A/D converter board and a terminal. The computer controller was a stand-alone single board microcomputer which was programmable in BASIC. The terminal and the computer controller were connected through RS232C ports. The terminal permitted programs to be uploaded to the computer controller and data to be downloaded to the terminal.

### Description of the controller sequences

The control parameters used during the experiments are summarized in Table III. The controller operated by continuously following a series of three phases. At the onset of each run, the bypass damper was completely closed so that all the supply air was routed through the defrosted core of the exchanger. The temperature rise of the supply air combined with this maximum air flow rate gave a measured rate of heat transfer which was taken to represent the maximum thermodynamic potential of the system (MTP).

After the MTP measurement, and again once each cycle, a defrost was initiated by diverting more and more outside air

Table III. Control parameters for defrost control system

Parameter	Value
Control error for the cold air stream temperature change necessary to initiate a defrost ( $^{\circ}\text{C}$ )	-2.5
Exhaust air stream set point temperature ( $^{\circ}\text{C}$ )	2.5
Control gain ( $^{\circ}\text{C}^{-1}$ )	0.02
Defrost set point temperature ( $^{\circ}\text{C}$ )	0.0
Time interval between control actions (min)	6.0

through the bypass until the heat exchanger core temperature rose to a defrost set point temperature ( $^{\circ}\text{C}$  in these tests). The supply air flow rate was modulated using proportional control on the assumption that in some cases the bypass damper would not need to be completely open during defrost and thus that some minimum rate of heat recovery could be maintained even during defrost.

Once the heat exchanger had been defrosted, the flow of cold air through the heat exchanger core was increased until the air temperature at the exit from the exhaust air passages was within  $1.0^{\circ}\text{C}$  of a set point temperature ( $2.5^{\circ}\text{C}$  in these tests). This was done by moving the dampers with proportional control action. The maximum supply air flow rate was not automatically selected in this phase because it was expected that if the exhaust air exit temperature dropped below  $0^{\circ}\text{C}$  the exhaust air passages would quickly become blocked due to ice accumulation. Also, since the same experiments were used to validate a mathematical model of a frosting heat exchanger (Bantle 1986), ice accumulation had to be avoided. Computer simulations of the controller operation predicted that selecting an exhaust air temperature set point of  $2.5^{\circ}\text{C}$  would ensure that the exhaust air temperature did not go below  $0^{\circ}\text{C}$  before a defrost was initiated.

The last phase of the controller operation involved monitoring the temperature change of the supply air. During this phase the mass flow rate of the cold air stream was constant; hence, its temperature change was a direct measure of the heat transfer rate. The maximum temperature change (and maximum heat transfer rate) occurred at the start of this phase and both decreased as frost accumulated. When the temperature rise of the supply side air had dropped off by a preset amount ( $2.5^{\circ}\text{C}$  in these tests), a defrost was initiated and the control cycle was repeated. The magnitude of the drop in supply side temperature boost before defrosting controls the amount of frost accumulation, and therefore controls the reduction in exhaust side air flow rate that occurs before defrosting. A set point of  $2.5^{\circ}\text{C}$  was selected because the computer simulations indicated that a decrease in the temperature boost of  $2.5^{\circ}\text{C}$  could occur before the exhaust air flow rate decreased by more than 10% compared to the flow rate through a defrosted core.

The time interval between control actions was chosen on the basis of preliminary experiments with the heat exchanger while the control gain was chosen based on the results of computer simulations (Bantle et al. 1987). The preliminary experimental measurements indicated that, at rated flow, the thermal time constant of the heat exchanger was approximately 6 min. The simulation indicated that a control gain of  $0.02^{\circ}\text{C}^{-1}$  would result in quick control action without significant overshoot.

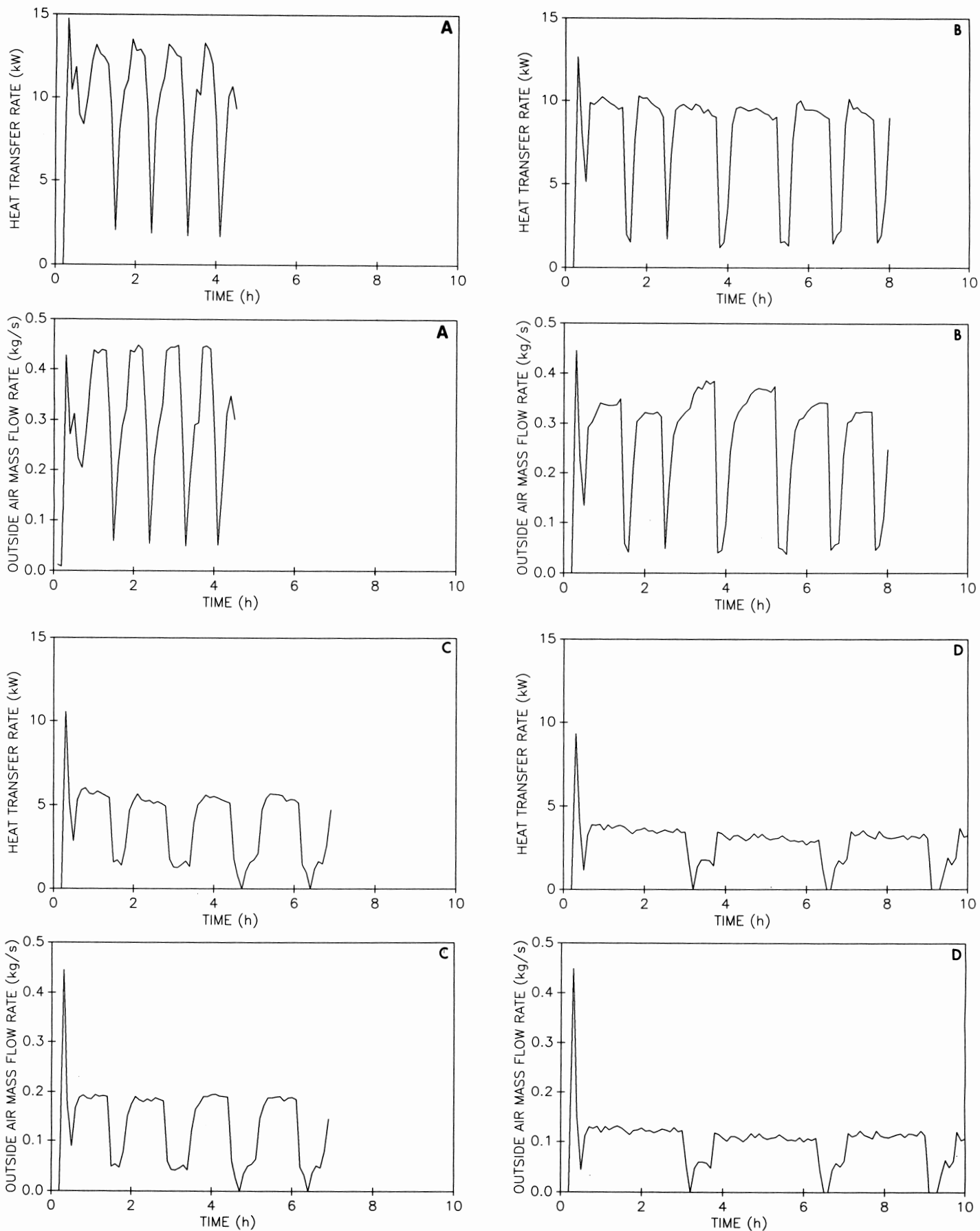


Figure 5. Performance of heat exchanger: (A) Run 1, (B) Run 2, (C) Run 3, (D) Run 4.

**Table IV. Heat exchanger performance using defrost control**

Run	Maximum thermodynamic potential (MTP)	Maximum heat transfer rate between defrosts		Time-averaged heat recovery rate (TAHRR)		Percent time supply air flow rate constant
	(kW)	(kW)	(% of MTP)	(kW)	(% of MTP)	
1	14.7	13.4	91	8.6	59	35
2	12.7	10.0	79	6.4	50	56
3	10.6	5.7	54	3.7	35	43
4	9.3	3.7	40	2.8	30	74

**RESULTS AND DISCUSSION**

Results from the four runs are shown in Fig. 5. For each run, one graph shows air flow rate while the other shows the heat transfer rate during a few cycles of heat recovery and defrost. In each of the heat recovery graphs, there is a sharp spike at the beginning of the run which gives the maximum thermodynamic potential (MTP) of the heat exchanger for that particular set of air conditions. In each run the heat recovery returned to almost the identical rate after each defrost. The length of the heat recovery period was approximately the same in each cycle of a run, but differed considerably from one run to another because of differences in the entering air conditions. The graphs show dramatic differences in air flow rates between runs, illustrating the responsiveness of the controller. When less heat was available in the exhaust air, due either to lower temperature or lower RH, the maximum flow rate of fresh air that was required to cool the exhaust air to 2.5°C was also less. The maximum fresh air flow rate which was selected by the controller for achieving the exhaust air setpoint temperature was approximately 145%, 110%, 60%, and 40% of the exhaust flow rate in Runs 1 to 4, respectively.

The graphs also show that heat recovery did not necessarily drop to zero during defrost. In Runs 1 and 2, defrost was accomplished without completely shutting off the fresh air supply. By contrast, for Runs 3 and 4, less heat was available in the exhaust air so it was necessary for the controller to completely close off the cold air to raise the core temperature above 0°C and obtain defrost. Consequently, some heat was recovered even during defrost in Runs 1 and 2, but not during Run 4.

Table IV summarizes the effect of exhaust air temperature and relative humidity on the heat exchanger performance. Decreasing either the temperature or the relative humidity of the exhaust air decreased both the MTP and the time-averaged heat recovery rate (TAHRR). Decreasing the exhaust air temperature or relative humidity while maintaining a constant exhaust temperature set point (2.5°C) also decreased the maximum supply air flow and the maximum heat transfer rate between defrosts.

**Opportunities for parameter optimization**

The heat-transfer-based frost controller was conceived and developed in anticipation that it could maximize the TAHRR of the heat exchanger. Expressed as a fraction of MTP, the TAHRR in the four runs varied from 0.30 to 0.59. Examination of the data from the runs and comparison of the measured heat recovery curves to an idealized heat recovery curve (Fig. 6)

suggests that higher heat recoveries could have been achieved by optimizing the values of the control parameters. With an optimized controller, the TAHRR will be maximized.

The heat recovery curves for Runs 3 and 4 show that the defrost was prolonged compared to the idealized situation. The prolonged defrosts were caused by the nonlinearity of the bypass damper. Table V, which gives results for the second full cycle in Run 3, shows that despite the core being above 0°C and defrosted at 3.1 h, it was 0.4 h before a significant increase in the supply air flow rate occurred. The data show that the bypass damper system was being correctly moved but because of the nonlinearity of the damper system the flow rate did not change proportionally. If control had been exercised directly over the flow rate rather than over damper position, the defrosts would have been shorter and the TAHRR would likely have been greater for Run 3.

The data from Run 3 also can be used to highlight the effect of the exhaust air temperature set point. Following defrost, the supply air flow rate was increased until the exhaust exit temperature was within 1°C of the 2.5°C control setting. The maximum supply air flow rate finally reached was 0.19 kg/s but it would have been larger if the exhaust air temperature set point had been lower. The value of 2.5°C was selected originally to provide a safety margin so that the exhaust air temperature would never fall below freezing. These experiments showed, however, that once the supply air flow rate was stabilized, the exhaust air temperature either remained constant or increased slightly. Therefore, the exhaust temperature set point could have been reduced to near 0°C without the fear of ice accumulation in the heat exchanger core. Whereas reducing the exhaust temperature set point would increase the rate of heat transfer, the rate of frost formation would also increase. Further simulations and experiments are required to determine the optimum value for the exhaust temperature set point.

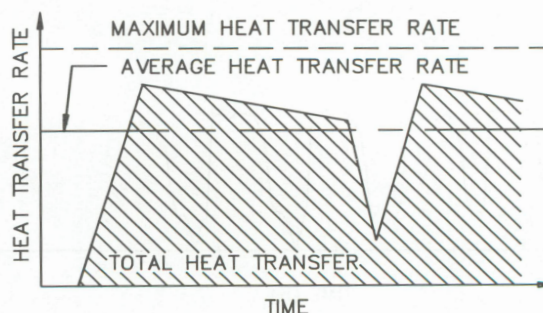


Figure 6. Idealized heat recovery curve for a frosting heat exchanger.

**Table V. Data for the second cycle in Run 3**

Time (h)	Exhaust exit temp. (°C)	Supply exit temp. (°C)	Core temp. (°C)	Supply air flow (kg/s)	Damper position (steps)
2.6	3.5	1.9	-16.2	0.187	142
2.7	3.7	1.6	-17.1	0.184	142
2.8	3.7	1.2	-17.8	0.181	62
2.9	7.4	5.9	-4.4	0.060	38
3.0	8.1	7.6	-0.7	0.043	30
3.1	8.4	8.4	3.8	0.042	54
3.2	8.5	8.2	3.4	0.046	78
3.3	8.1	8.1	2.7	0.052	100
3.4	8.5	8.2	3.3	0.042	124
3.5	5.8	6.6	-7.3	0.121	136
3.6	3.9	3.6	-12.9	0.164	140
3.7	3.5	3.1	-14.6	0.176	144
3.8	3.1	2.4	-16.7	0.190	144
3.9	2.8	1.5	-17.6	0.190	144

The effect of the controller gain and the time step between control actions was illustrated in Run 2. Data for the third cycle from Run 2 are given in Table VI. These data show that the controller took a very long time to reach the heat transfer monitoring phase. The defrost was complete at 3.9 h but the steady air flow phase was not reached until 4.6 h. Had the control gain been smaller and the time step larger, or if the controller had been operating in a region where the flow rate was less responsive to a change in damper position, the controller might never have reached the heat transfer monitoring phase. If a stable air flow phase had not been reached, then no defrost would have been scheduled and the core would have frozen up. This example illustrates the need to ensure that the gain is high enough and the time step small enough to ensure that each of the three phases of the cycle are reliably set.

**Table VI. Data for the third cycle in Run 2**

Time (h)	Exhaust exit temp. (°C)	Supply exit temp. (°C)	Core temp. (°C)	Supply air flow (kg/s)	Damper position (steps)
3.6	3.5	0.1	-21.4	0.379	264
3.7	3.4	-0.6	-22.1	0.385	96
3.8	11.7	8.2	-3.5	0.040	76
3.9	13.0	12.8	4.6	0.045	118
4.0	13.0	14.3	3.2	0.098	160
4.1	6.2	10.2	-12.2	0.243	246
4.2	4.0	6.6	-16.6	0.302	252
4.3	3.7	4.8	-17.8	0.323	256
4.4	3.6	3.5	-18.6	0.334	260
4.5	3.4	2.4	-19.4	0.342	262
4.6	2.8	1.3	-20.0	0.359	262

The amount of heat transfer degradation permitted before a defrost was initiated was determined by the control error for the supply air temperature change. If the amount of heat transfer degradation permitted is too small, defrosts will be scheduled more often than necessary and the TAHRR will be less than the maximum that could be achieved under more optimal control. On the other hand, if too much frost is allowed to accumulate between defrosts, the exhaust air flow rate will decrease excessively. If the exhaust air flow rate falls far enough, the

building ventilation rate may become too small for removal of contaminants. In these experiments, a value of  $-2.5^{\circ}\text{C}$  was selected for the control error for the supply air temperature change. This value was chosen based on simulation predictions that the exhaust air flow rate would not be reduced by more than 10% and that a reasonable TAHRR would be achieved. The data indicated that the percent reduction in the exhaust air flow rate during the heat transfer monitoring phase was less than 4% for all runs except Run 2. In that run, the larger reduction was probably due to the difficulty the controller had in reaching the heat transfer monitoring phase. The results indicated that the decline in the heat transfer rate during the heat transfer monitoring phase of the cycle was nearly 9% in all the runs. These results suggest that a larger control error could have been used to increase the TAHRR without seriously impeding the exhaust air flow rate.

### Implementation of the heat recovery maximizing controller

The experimental measurements demonstrated that the controller operated well with the control strategy that had been developed. Prior to implementing this strategy, several factors should be considered:

1. The bypass damper should be calibrated so that the control algorithm can be based on step changes in the air flow rate rather than steps in the damper position.
2. Further investigation is required to establish how much lower than  $2.5^{\circ}\text{C}$  the exhaust air set point can be before excessive amounts of ice accumulate in the heat exchanger core. Lowering the set point could significantly increase the average heat recovery.
3. Further optimization of the control gain and time step could probably provide faster response without loss of stability and with some increase in heat recovery. Calibration of the damper is necessary before this can be done.
4. The length of the heat recovery phase and the amount of reduction of the exhaust air flow rate are both affected by the control error for the cold air stream temperature change necessary to initiate defrost. Observations suggest that a larger control error could be applied, but the effect of this on frost accumulation and time required to defrost must be determined to optimize this control parameter.
5. Implementing this control strategy requires measurement of temperatures at four locations and calibration of the damper. Under some circumstances a control cycle can take several hours, and outdoor temperature could change by several degrees. The control algorithm needs to include provision for this change in temperature so that the change in the rate of heat recovery can be calculated.

### Comparison with other control strategies

If the option of preventing frost formation is chosen, the core temperature must remain at or above  $0^{\circ}\text{C}$  at all times. For each of the four experimental runs, using linear interpolation and only considering measurements made after the heat exchanger had been defrosted, the heat transfer rate was calculated for a core temperature of  $0^{\circ}\text{C}$ . Table VII summarizes these calculations and compares them to the TAHRR when the defrost cycle was used. In all the runs, the TAHRR with the defrost control system

exceeded the heat transfer rate that could be achieved if the core temperature was kept just above freezing. The heat recovery advantage of the defrost control system would be even larger if all of the control parameters were optimized.

**Table VII. Comparison of the MTP, TAHRR, and the heat transfer for a core temperature of 0°C**

Run	MTP (kW)	TAHRR (kW)	Heat transfer for core temperature 0°C (kW)
1	14.7	8.6	8.1
2	12.7	6.4	4.9
3	10.6	3.7	2.7
4	9.3	2.8	0.6

The timed defrost system can be re-examined relative to Eq. 1, the frost growth equation developed by O'Neal and Tree (1984).

$$x_f = 0.466 \left( \frac{t}{1 \text{ hour}} \right)^{0.663} Re^{0.393} \left( \frac{T_o - T_p}{T_o} \right)^{0.705} \left( \frac{W_a - W_o}{W_o} \right)^{0.098} \quad (1)$$

When a timed defrost cycle is used, the only factor that is considered is time. However, Eq. 1 and the experiments reported in this paper clearly show that the accumulation of frost is very much affected by the supply air temperature, the exhaust air temperature and relative humidity, and the air flow rates on both sides of the core. Because the timed defrost system considers only time, the TAHRR for that control system is expected to be less than for the heat transfer-based defrost controller developed in this project.

Pressure-based defrost systems address the problems of scheduling defrosts in a very direct manner; i.e., on the basis of the effect of the frost formation on the exhaust air flow rate. However, for maximization of the TAHRR, a control strategy is required that will control the rate of accumulation of frost, not just the level of frost accumulation that will trigger a defrost. Furthermore, pressure-based systems will not automatically adjust to fouling of the core or to any other factors that might cause a change in the pressure characteristics of the heat exchanger system.

For each of the four runs, the pressure drop across the exhaust side of the heat exchanger with no frost accumulation was 92 Pa. The maximum increase in pressure drop which was measured in each run is shown in Table VIII. Since the pressure drop was measured every 30 m in the tests, the maximum pressure drop reported in the table may not correspond to the most extreme condition. Also shown in Table VIII are data for the average amount of condensate released during a defrost cycle for Runs 2, 3 and 4. The weigh scale failed during Run 1 and no data on condensate were obtained.

**Table VIII. Pressure drop and condensate release data**

Run	Increase in exhaust-side pressure drop due to frost accumulations (Pa)	Average condensate release per defrost cycle (kg)
1	107	-
2	197	2.47
3	132	2.39
4	105	0.46

The pressure drop data indicate that a pressure-based defrost controller would have scheduled defrosts differently than did the experimental controller used in these experiments. For example, if the change in pressure drop required to initiate a defrost was 130 Pa, defrosts would have been scheduled less often in Run 1 and Run 4, and more often in Run 2. This result indicates that, in a system with a pressure-based defrost controller, the reduction in heat transfer that occurs before each defrost can be expected to vary widely depending upon supply and exhaust air conditions.

Condensate release and pressure drop, the two measures of the extent of frosting in the heat exchanger, were not correlated. The amount of condensate released during a Run 4 cycle was much less than would have been expected given the pressure drop data and the condensate data for the other runs. This result indicates that there were differences among the runs in terms of where and how the frost accumulated within the heat exchanger core and thus in terms of how the rate of heat transfer was affected and how the blockage to airflow occurred. More research is needed on the dynamics of frost accumulation in a frosting core before optimization of the set-point pressure drop for a pressure-based controller can be realized.

## SUMMARY AND CONCLUSIONS

The objective of this project was to develop and test a control algorithm in which the rate of heat transfer is monitored and controlled, and in which a defrost is scheduled on the basis of a preset decrease in the rate of heat transfer. Such a heat recovery maximizing controller was built and tested and was found to operate satisfactorily. The control algorithm consisted of three distinct phases (setting exhaust temperature, monitoring heat transfer, and controlling the defrost).

Four control parameters that are critical to the design of a heat recovery maximizing controller were identified: (a) the gain used in the proportional control phases of the cycle (i.e., moving to and from a defrost); (b) the decrease in heat transfer rate (or supply temperature change) permitted before triggering a defrost; (c) the minimum exhaust-side exit temperature allowed (and hence the maximum supply flow rate and heat transfer rate permitted immediately following a defrost); and (d) the time step between control actions. Further work is required to optimize the selection of values for these control parameters.

The instrumentation and equipment required to implement the heat recovery maximizing frost control strategy consists of sensors to measure the supply air temperature at the core inlet and outlet, the exhaust air exit temperature and the core temperature, a damper and stepper motor, and a microprocessor. The control algorithm should be based on step changes in the supply air flow rate rather than on step changes in the damper position.

Compared to alternative heat exchanger control systems, the experimental control system offers greater potential for optimizing the time-averaged rate of heat recovery for a heat exchanger operating under dynamic environmental conditions. Even though the controller was not optimized, the control system involving a defrost cycle increased the time-averaged heat transfer rate compared to that which would have been attained with a control system in which, to prevent frost formation, the core temperature was maintained at 0°C.

#### ACKNOWLEDGMENTS

Acknowledgment is made to the Financial contributions to this project by Agriculture Canada and by NSERC through Operating Grants to E. Barber. The authors also gratefully acknowledge the assistance and interest of personnel at the Machinery Institute at Humboldt, Saskatchewan where the experiments were conducted.

#### REFERENCES

BANTLE, M. R. L. 1986. Prediction and control of frost formation in an air-to-air heat exchanger. Unpublished M.Sc. Thesis, Agric. Eng. Dept., University of Saskatchewan, Saskatoon, SK.

BANTLE, M. R. L., E. M. BARBER, and R. W. BESANT. 1987. A mathematical model of a plate type air-to-air heat exchanger operating under frost forming conditions. Proc. 1987 Int. Symp. on Cold Regions Heat Transfer. K. C. Chen, V. J. Lunardini, and N. Seki, eds. Am. Soc. Mech. Eng., New York, NY. pp. 195-205.  
 HODGKINSON, D.G. and D. SMALL. 1984. Field evaluation of a single-plate air-to-air heat exchanger for livestock buildings. Paper No. 84-403, Can. Soc. Agric. Eng., Ottawa, ON.  
 MEYER, D. J., H. B. MANBECK, and P. N. WALKER. 1983. Performance of a polytube heat exchanger in a farrowing-nursery building. Paper No. 83-4563. Am. Soc. Agric. Engrs., St. Joseph, MI.  
 O'NEAL, D. L. and D. R. TREE. 1984. Measurement of frost growth and density in a parallel plate geometry. ASHRAE Trans. 90(2A):278-290.

#### APPENDIX A. NOMENCLATURE

Re = Reynolds number (based on hydraulic diameter)  
 t = time (h)  
 $T_o$  = freezing temperature of water (K)  
 $T_p$  = plate temperature (K)  
 $W_a$  = humidity ratio of the air stream  
 $W_o$  = humidity ratio of saturated air at 0°C  
 $x_f$  = thickness of the frost layer (mm)